

Polarization of Fe(001) covered by MgO analyzed by spin-resolved x-ray photoemission spectroscopy

M. Sicot, S. Andrieu, P. Turban, Y. Fagot-Revurat, and H. Cercellier

Laboratoire de Physique des Matériaux, UMR7556 CNRS/Univ. Nancy I, B.P. 239, F-54506 Vandoeuvre, France

A. Tagliaferri, C. De Nadai, and N. B. Brookes

ESRF, B.P. 220, F-38043 Grenoble Cedex, France

F. Bertran and F. Fortuna

LURE, B.P. 34, F-91898 Orsay, France

(Received 26 March 2003; revised manuscript received 29 August 2003; published 6 November 2003)

Single-crystalline (001) Fe thin films were prepared by molecular beam epitaxy and covered by epitaxial MgO barriers. The MgO growth was confirmed to be layer by layer as shown by reflection high-energy electron diffraction, which allowed us to prepare Fe films covered by only two atomic planes of MgO for spin polarization measurements. On the one hand, regular x-ray photoemission spectroscopy measurements evidenced a weak hybridization between Fe and O. Moreover, a large Fe magnetic moment at the interface with MgO was shown by x-ray magnetic circular dichroism measurements. These two observations are in agreement with theory. On the other hand, we show that the Fe density of states can be measured by photoemission through the oxide barrier, since the oxide valence band only starts at 4 eV below the Fermi level. Spin-resolved x-ray photoemission measurements performed at ESRF allowed us to demonstrate that the electrons emitted from the (001) Fe layer through the barrier are polarized. A polarization fully integrated in k space and corrected from remanence near 42% was measured.

DOI: 10.1103/PhysRevB.68.184406

PACS number(s): 75.70.Cn, 85.75.-d, 79.60.Jv, 73.40.Gk

I. INTRODUCTION

For many years, a lot of work has been dedicated to the study of magnetic tunnel junctions (MTJ's) due to their large potential in applications especially in spintronics.¹ A MTJ is constituted of two magnetic layers separated by an oxide layer, with a thickness close to the nanometer. Due to this low thickness, electrons pass through the oxide barrier by tunneling.² Moreover, the spin state of a conducting electron is conserved during its transport from one electrode to the other through the barrier.³ The different concepts of new spintronic components were based on this spin conservation.⁴ Indeed, if we imagine that in the first electrode all the conducting electrons are polarized (with a spin up), this spin-up current passes through the barrier only if some spin-up empty states exist in the second electrode. Thus, in the ideal case of two 100%-polarized electrodes, a current takes place if both magnetization directions are parallel and becomes equal to zero if the magnetization directions are antiparallel.

In practice, the usual ferromagnetic materials used in MTJ's (Fe, Co, Ni, associated compounds, ...) are not fully polarized. However, the density of electronic states at the Fermi level for spin up and spin down are not equal, leading to a nonzero polarization. In that case, an asymmetry of the current (or resistance R) is observed for the parallel and antiparallel magnetic configurations of the electrodes which lead in first approximation to the so-called tunneling magnetoresistance (TMR) defined as³

$$\text{TMR} = \frac{\Delta R}{R} = \frac{2P_1P_2}{1 - P_1P_2}, \quad (1)$$

where P_1 and P_2 are the polarization of each electrodes. The higher the polarizations, the better the TMR is. This is the reason why a lot of studies have been dedicated to the determination of the polarization of magnetic materials. One way to measure directly the polarization of a material is to perform spin-resolved photoemission spectroscopy near the Fermi level. Such a measurement has to be performed in vacuum on a well-controlled contamination-free surface in order to detect electrons that only come from the material. Indeed, if another material is present, the density of states of this former material will be included in the measurement. However, the polarization of a free surface is *a priori* not the pertinent polarization to predict the TMR. Indeed, as the polarization is fixed by the density of states of the electrons at the highest energy levels, near E_F , these electrons also participate in the chemical bonding with a layer deposited on it and especially with an oxide. Consequently, there is absolutely no reason that the polarization of a material determined on its free surface remains the same when it is covered by the oxide barrier.

The first goal of this study is to measure the polarization of a magnetic material covered by the oxide barrier—that is, the pertinent polarization for MTJ's. The basic idea is the following. The Fermi level of an oxide is in the gap (more precisely in the middle of the gap if there is no impurities). Consequently, from the Fermi level down to the highest energy of the valence band there is no density of states if the oxide is pure and if no surface states exist (indeed, impurities or surface states generate some new energy levels located in the oxide gap). If this is the case, it becomes possible to measure the density of state of the magnetic layer below the oxide barrier, from the Fermi level down to the beginning of

the oxide valence band, and consequently to measure the polarization of the electrode covered by the oxide. In order to test this idea, we had to choose an appropriate electrode/oxide system. This choice is actually limited by some intrinsic constraints. On the one hand, as the photoemission process leads to the emission of an electron from the analyzed material to vacuum, the escaping depth of the electrons through the material is equal to a few atomic planes. Consequently, an oxide barrier thickness as small as possible has to be chosen in order to minimize the attenuation of the electronic emission from the electrode through the oxide barrier (exponential with the thickness). On the other hand, the electrode surface has to be totally covered by the oxide barrier. Indeed, if some electrode surface regions are not covered by the oxide, the photoemitted electronic current coming from these regions will be much higher than those coming from the regions covered by the oxide. The epitaxial Fe/MgO(001) system is appropriate since the MgO growth on Fe(001) is layer by layer.^{5,6} This behavior allows us to minimize the MgO layer thickness down to two atomic planes.

This study was secondly motivated by theoretical predictions about electronic properties of the Fe/MgO interface: a small hybridization between Fe and MgO is expected, leading to a high Fe magnetic moment at the interface, like on the free Fe surface.⁷ Such an improved magnetic moment at the electrode/oxide barrier interface should lead to an improved polarization. In addition, no minority-spin transport is expected at the Γ point in the Brillouin zone.^{8,9} Consequently, a high polarization rate is expected along the [001] crystallographic direction.

The samples were prepared by molecular beam epitaxy (MBE). The growth, structure, and chemical aspects were characterized by scanning tunneling microscopy (STM), reflection high-energy electron diffraction (RHEED); and Auger and x-ray photoemission (XPS) regular spectroscopies. The electronic properties near the Fermi level were characterized by high-resolution ultraviolet photoemission spectroscopy (HR-UPS). The magnetic behavior of the Fe layer near the interface was studied by using x-ray magnetic circular dichroism (XMCD) at saturation at LURE (on SU23 beamline at SuperAco ring) and in remanence at ESRF, and the spin polarization by spin-resolved x-ray photoemission spectroscopy (SR-XPS) at ESRF (on ID8 beamline).

II. EXPERIMENTAL DETAILS

The sample preparation was processed at the LPM in Nancy. The Fe layers were grown on MgO(001) clean single-crystalline substrates prepared *ex situ* and *in situ* outgassed up to 1200 K. Auger electron spectroscopy (AES) allowed us to check that there were no impurities on the surface. In particular, no C contamination was detected. Fe was sublimated by using a Knudsen cell heated at 1500 K, leading to a growth rate of 1.8 nm/min. The Fe layers were 100 nm thick. They were grown at room temperature and heated up to 800 K after the deposition in order to smooth the surface. Again, no C nor O contamination was detected by AES. The MgO was evaporated at a growth rate around 1 nm/min by using an electron gun. The MgO layer was deposited at room

temperature. Regular XPS measurements were also performed at the $L_{2,3}$ Fe edge using an Al anode in order to get some information about the hybridization between Fe and MgO at the Fe/MgO interface. Finally, in order to demonstrate that the measurement of Fe polarization through MgO was possible, we performed HR-UPS measurements by using a Scienta equipment (SES200) with a He II UV source ($h\nu=40.8$ eV). It should be noted that the integrated photoemission spectra for this energy are close to the density of states (DOS) of Fe (convoluted with the Fermi-Dirac distribution) as generally the case for $3d$ metals.

Since the samples were prepared in the MBE chamber in Nancy and measured at LURE and ESRF, an exposure to air was necessary, leading to some risk of degradation of the samples surface. In order to avoid this problem, the samples dedicated for XMCD measurement at LURE were simply capped by a 2–3-nm-thick MgO epitaxial layer. For photoemission measurements, the capping was a 100-nm-thick Sb layer. The samples were always transported in a N_2 atmosphere, the exposition of the samples to the air being limited to less than 1 h. We have checked that a heating up to 700 K was sufficient to desorb almost all the Sb layer. However, about 1 ML (monolayer) of Sb still remained on the surface and a heating up to 800 K was thus necessary to eliminate it. We consequently checked that the Fe/2 ML MgO system was not destroyed by such a heating process. For this purpose, XPS spectra were collected just after the MgO growth at room temperature (RT) and after several heating up to 850 K. No difference was observed between the spectra. This means that no interdiffusion took place between Fe and MgO, when MgO is firstly deposited at RT.¹⁰ The experimental process at the ESRF was thus the following. First, the Sb capping layer was desorbed using heating temperatures up to 800 K. Second, the chemical and crystallographic quality of the surface were checked by AES and/or XPS and low-energy electron diffraction (LEED). No C contamination was observed after the process, and a sharp 1×1 surface structure was observed by LEED.

At LURE, the XMCD measurements were performed by using a fixed circular polarization and by flipping the applied magnetic field. The circular polarization rate was 40%, and the angle between the surface and the x-ray beam was 45° . Both remanent and saturated magnetization were measured by applying magnetic fields up to 1 T. The measurements were performed around 20 K. At ESRF, the XMCD and SR-XPS measurements were performed in the remanence mode. Both applied magnetic field and x-ray polarization were flipped before the absorption measurements. Four absorption spectra were thus recorded and combined, which allowed us to eliminate some asymmetry due to the apparatus as often observed. The x-ray circular polarization rate was 99%. The magnetization was calculated by using the sum rules on XMCD measurements with the process proposed in Ref. 11. The SR-XPS measurements were performed in the same conditions, and the polarization was determined using the process described in Ref. 12. The SR-XPS experiments were performed with an incident photon energy of 500 eV. Like in HR-UPS measurements, the photoemission spectra obtained

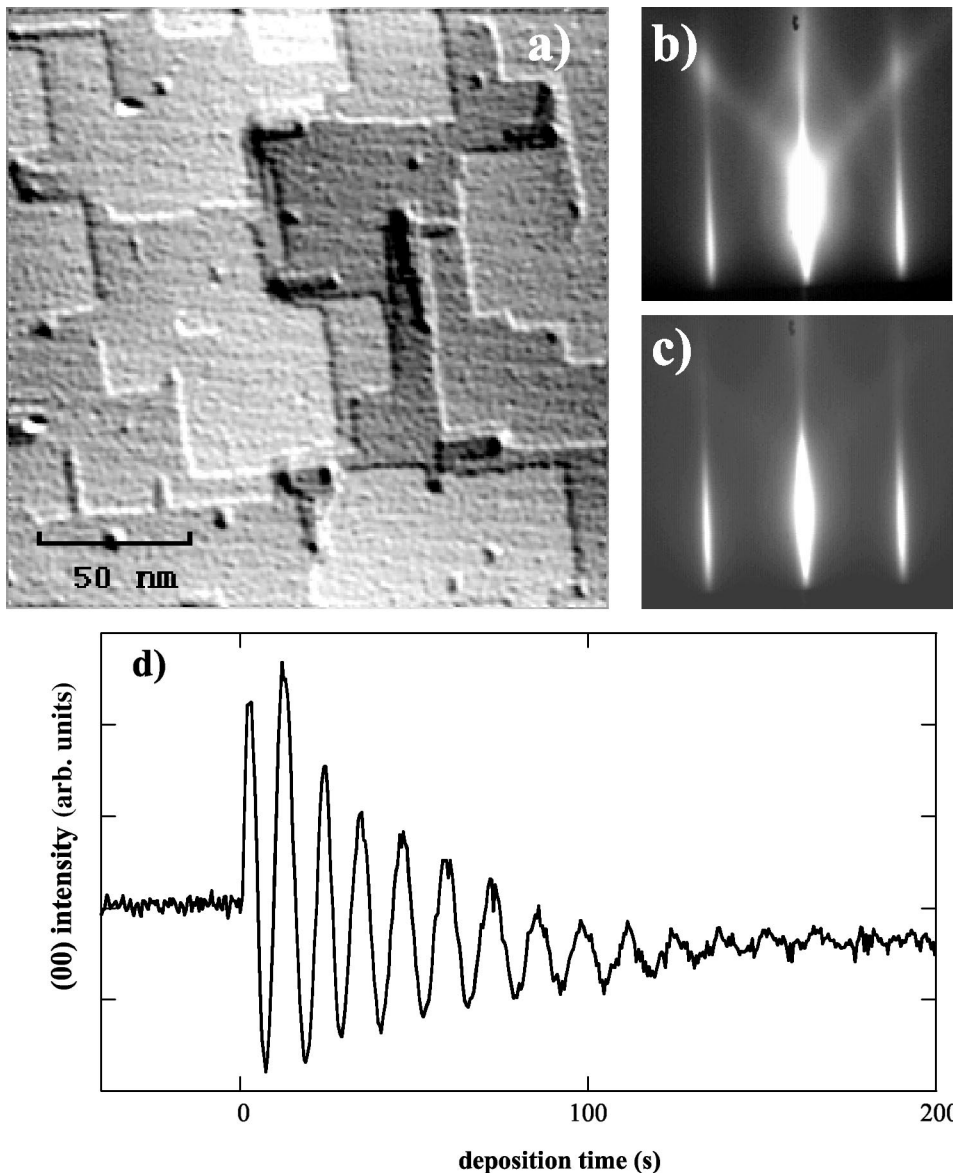


FIG. 1. Illustration of the Fe/MgO(001) system quality: (a) $200 \times 200 \text{ nm}^2$ STM image of the starting (001) Fe buffer layer, (b) RHEED patterns along the [11] azimuth of the square lattice of Fe and (c) of the 2-ML-thick MgO layer, and (d) RHEED oscillations observed on the (00) streak during the MgO growth on Fe at room temperature.

on Fe are similar to the Fe DOS. The total resolution during the experiments was 0.28 eV. All the electrons emitted by the surface with an angle of $\pm 20^\circ$ were collected. Consequently, the full density of state was measured (integrated in k space). The spin detection was ensured by using a Mott detector.¹³ The polarization was calculated using a Sherman function equal to 0.142 determined on a CuO reference. The Fermi level was accurately determined by measuring a gold reference sample in electrical contact with the sample. In both experiments at LURE and ESRF, the magnetic field was applied along the (100) Fe easy axis in the surface plane.

III. EXPERIMENTAL RESULTS

A. Growth and structure

We first would like to show that the Fe/MgO(001) system is a model system for our purpose, concerning both the morphologic, crystallographic, and chemical aspects. The Fe buffer layer preparation allowed us to get model (001) Fe

surfaces, with large terraces as shown by STM and sharp 1×1 surface structure as observed by RHEED (Fig. 1).¹⁴ It should be noted that such Fe surfaces prepared by heteroepitaxy on MgO(001) are not as smooth as Fe whisker surfaces.⁶ Four level of terraces are present on this image, leading to a height difference of 4 ML between the lowest and highest terraces. However, the height of an individual step is 1 ML. At least, due to some emerging dislocations coming from the misfit between the MgO substrate and Fe layer, some steps of 2 ML height are sometime present. Nevertheless, such a surface quality is sufficient to our purpose, and the heteroepitaxial Fe/MgO(001) solution is of technological interest compared to whiskers in order to realize magnetic tunnel junctions.

The RHEED patterns (Fig. 1) observed on the deposited MgO layer confirmed the epitaxial relation (001) [110] MgO || (001) [100] Fe. RHEED oscillations typical of a layer-by-layer growth mode were observed (Fig. 1), which allowed us to control accurately the time needed to complete one

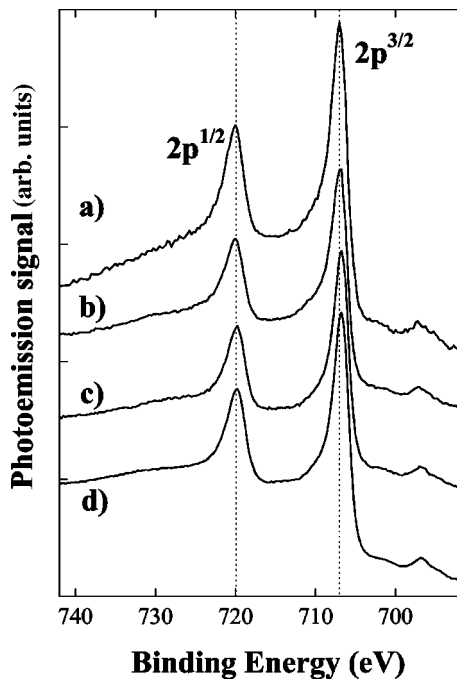


FIG. 2. XPS spectra performed at room temperature on (a) V(50 nm)/Fe(2 ML), (b) same sample covered by 2 ML MgO, (c) same as (b) heated at 570 K, and (d) thick Fe layer.

atomic layer. It should be noted that these RHEED oscillations are easy to see with the naked eye: the amplitude of the oscillations is as large as 2/3 of the full scale of the charge-coupled device (CCD) camera. We have also checked that the AES spectra performed on the deposited MgO layers and on the MgO substrate were exactly the same. This indicates that the stoichiometry of the deposited MgO layer is correct, in agreement with the results reported in Ref. 15. Concerning the Fe and MgO lattices coincidence, it seems to be well established that the Fe atoms sit above the O ions.¹⁶ Such an oxygen on-top position was also found to be more stable than the Mg in-top position in the calculations by Li and Freeman.⁷ Concerning the Fe-O hybridization, these authors also predicted a very low electronic transfer from Fe to O ($0.3e^-$). As a strong Fe-O hybridization like in FeO and Fe₂O₃ leads to strong modifications of the photoemission Fe 2*p* core levels,¹⁷ this result may be easy to test by XPS. For this purpose, we performed XPS experiments (with the Al anode) first on a 2-ML-thick Fe layer grown at RT on a (001) V buffer layer, second on the same sample but covered by 2 ML of MgO grown at RT, and third on the same sample heated up to 570 K. These spectra were finally compared to the XPS spectra obtained on a thick Fe film. The results are shown in Fig. 2. No new satellite peaks and no chemical shift of the Fe 2*p* core levels were observed, which means that no FeO or Fe₂O₃ hybridization like took place. Moreover, the heating at 570 K did not change at all the XPS spectrum. This means that no interdiffusion between V, Fe, and MgO took place and that the Fe/MgO hybridization did not change. These results consequently support the analysis of Li and Freeman, even for temperatures up to 570 K. However, Meyerheim *et al.*¹⁸ interpreted their surface x-ray diffraction

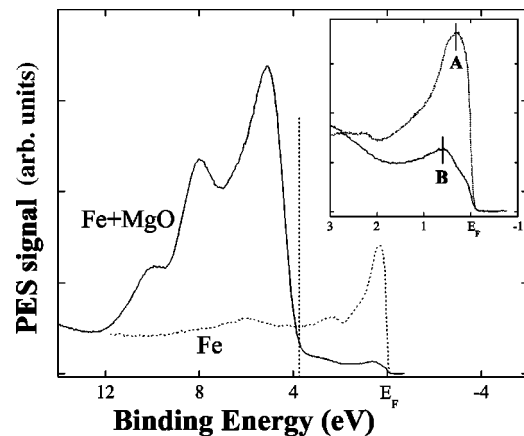


FIG. 3. High-resolution UPS spectrum performed at room temperature with He II source on a free (001) Fe surface and on a (001) Fe/3 ML MgO sample. In the inset is shown close-up of the photoemission signal coming from Fe with higher statistics for both samples.

experiments by the occurrence of a FeO layer at the interface. If such an FeO interlayer actually exists, our results clearly show that Fe and O are not hybridized like in bulk FeO.

B. Electronic properties

The HR-UPS experiments were performed to demonstrate both the ability of the technique to measure the Fe DOS through MgO and the Fe DOS modifications when covered by MgO. In Fig. 3 is shown a typical angle-integrated photoemission spectrum obtained on a (001) Fe layer covered by a 3-ML MgO layer. In order to compare this measurement with the free Fe(001) surface, a similar experiment was performed on the same sample after having removed the initial MgO layer (by Ar sputtering and annealing at 750 K). In the following, we discuss first the measurement performed on the free surface and second the spectrum's modifications with the MgO covering, both with an angular integration of $\pm 8^\circ$. We third discuss on the observations for an increasing angular integration.

The photoemission spectrum measured on the free Fe layer (dashed lines) is in perfect agreement with those obtained in the literature at the same excitation energy and angular integration range ($\pm 8^\circ$). In this system, numerous spectroscopic studies^{19–23} have shown that both the spin polarization and band spectral weight are strongly dependent on the range of angular integration used and on the energy of the excitation light. Close to the Fermi level, the main peak observed around 0.3 eV (denoted A in the inset of Fig. 3) is ascribed to spin-polarized *d* bands, as shown by the strong increase of the spectral weight observed by increasing the photon energy. The average energy position of this feature results from the *k* integration of a well-defined dispersive *d* band over $\approx 1/3$ of the full Brillouin zone around the Γ point due to the angular integration range. Previous normal emission spin-polarized photoemission spectroscopy (PES) measurements (at the Γ point) performed at low energy ($h\nu \approx 50\text{--}70$ eV) have demonstrated the strong minority-spin

character of this d band (for $E_B < 0.5$ eV), whereas the majority-spin band is deeper (for $E_B > 0.5$ eV).^{19–23} It should be noted that this contribution around 0.3 eV does not come from a surface state. Indeed, photoemission and scanning tunneling spectroscopy (STS) investigations of the free (001) Fe surface allowed us to identify surface state bands at Γ located on the one hand at 0.2 eV *above* the Fermi level and on the other hand at more than 2 eV *below* the Fermi level.^{24–26}

With the MgO covering, the situation is much different. First, we have observed on a thick MgO layer that the typical MgO DOS in the PES spectra starts around 4 eV below the Fermi level due to the strong insulating nature of the MgO thin film. Assuming a Fermi level lying in the middle of the MgO energy gap (7.9 eV), these results are in good agreement with the STM and UPS results already published.⁶ We consequently get a clearance of 4 eV below the Fermi level where the PES signal coming from MgO is zero. This is in this energy range that the DOS of the Fe layer below the MgO layer may be “seen.” For thinner MgO covering like in Fig. 3, a non-negligible DOS is actually observed inside the gap, which can be undoubtedly ascribed here to the Fe DOS measured through the MgO barrier. As the mean free path at this excitation energy is rather small, the photoelectrons are emitted from the last Fe layers. Thus the experimental Fe DOS measured here is mainly representative of the Fe/MgO interface. Note that this measured DOS remains unchanged with an annealing up to 900 K. Compared to the free Fe DOS, the low-energy 3-ML MgO/Fe DOS is strongly reduced close to the Fermi level and the main feature (denoted B in the inset of Fig. 3) appears now deeper (around $E_B \approx 0.6$ eV) compared to the Fe DOS of the uncovered Fe surface. It is thus natural to conclude to a strong reduction of the low-energy spectral weight mainly attributed to the dispersive feature in the $0.2 \text{ eV} < E_B < 0.5 \text{ eV}$ range for the free Fe. Therefore, this result gives clear experimental evidence that the electronic structure of the last Fe layer(s) involved in the MgO/Fe interface is locally different from the free (001) Fe. Moreover, due to the moderate k -integration range involved here, we can deduce that this spectral weight reduction concerns mainly the $k_{\parallel} \approx 0$ states. As long as these missing states are assumed to be spin polarized (of minority-spin character from Refs. 19–21), the consequence should be a strong positive polarization enhancement close to the Fermi level, especially for the normal emission electrons which are supposed to mainly contribute to the spin-polarized tunnel current.²⁷ This is in agreement with the calculations presented in Ref. 8.

In addition, we performed similar experiments (on the free Fe surface and on Fe covered by MgO), but with an increasing angular integration. On the one hand, we did not observe any noticeable modification of the Fe/MgO PES spectrum, still characterized by a peak (B) at 0.6 eV below E_F . On the other hand, the maximum feature (A) observed on the free surface progressively vanished and a spectrum similar to the Fe/MgO one was thus observed. These observations again confirm that the main modification of the PES signal of Fe when covered by MgO occurs around the Γ point.

To summarize, we first demonstrate the possibility to measure the Fe DOS through the oxide barrier by photoemission. Second, even if we could not go as far as to say that the minority-spin channel was destroyed around the Γ point as predicted (since the experiments were not spin resolved), these preliminary experiments allow us to confirm some strong modifications of the Fe DOS around the Γ point when covered by MgO as suggested by the calculations.

C. Magnetic properties

The magnetic properties of the Fe/MgO system were studied at LURE. The remanent magnetic moment was measured on a 100-nm-thick Fe film protected by a 3-nm MgO film. The remanent magnetization was found to be 94% of the saturated magnetization. Moreover, in order to determine the magnetic moment of Fe at the Fe/MgO interface, special samples were prepared. A model sample for this purpose should be one atomic Fe plane in between two MgO layers. However, the Fe growth mode is three dimensional on MgO. Consequently, we chose to grow the Fe layer on a V buffer layer since Fe grows layer by layer and keeps its bcc structure on V. The choice of V was also supported by the reduced magnetic moment of Fe in contact with V.²⁷ Indeed, since a large magnetic moment is predicted for Fe in contact with MgO,⁷ the XMCD signal should be greatly affected by replacing the Fe/MgO interface by the V/Fe interface. Finally, the Fe film thickness should not be too thin since the Curie temperature is well known to decrease with the thickness. Two samples were thus prepared on MgO substrates: $V_{50 \text{ nm}}/Fe_{6 \text{ ML}}/V_{3 \text{ ML}}/MgO_{2 \text{ nm}}$ and $V_{50 \text{ nm}}/Fe_{6 \text{ ML}}/MgO_{2 \text{ nm}}$. The 50-nm-thick buffer layers were first grown at RT and annealed at 1000 K. The Fe layers were grown at RT and annealed at a limited temperature equal to 500 K since we observed that Fe/V bulk interdiffusion starts at 670 K. The MgO and V overlayers were grown at RT. It should be noted that we are able to grow *V buffer layers without oxygen* on the surface as detected by Auger spectroscopy.²⁸ The XMCD signals measured at saturation (500 Oe was sufficient) on these layers were compared to the XMCD signal obtained on the thick Fe film taken as a reference. We consequently get three XMCD measurements as shown in Fig. 4, for three unknown parameters: the Fe moments at the interface with MgO and V and the escape depth λ of the electrons in Fe which defines the attenuation constant k of the absorption signal with the thickness as $k = \exp(d/\lambda)$. The absorption measurements and sum rule applications on these three samples are shown in Fig. 4. Assuming that the moment of only one Fe atomic plane is affected at the interfaces and that the absorption signal of one atomic plane is decreased by a factor of k^n when covered by n atomic planes, the isotropic absorption σ_0 and the absorption with right-left circular light $\sigma_{N/P}$ may be written as a function of the absorption for one atomic plane σ_1 . In the case of the first sample (thick Fe + MgO) we get

$$\sigma_0 = \sum_{n=0}^{\infty} k^n \sigma_1 = \frac{\sigma_1}{1-k}, \quad (2)$$

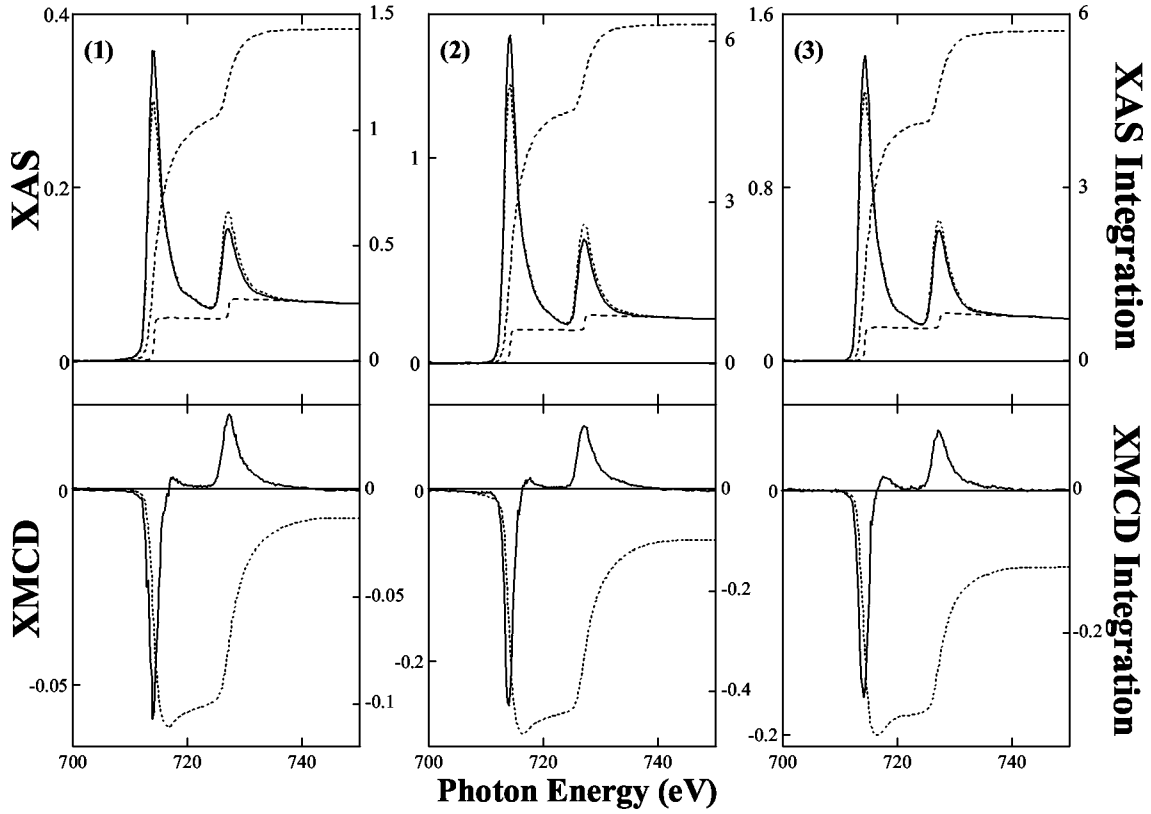


FIG. 4. Absorption and XMCD spectra (left scale) measured at 10 K on (1) Fe(100 nm)/MgO(3 nm), (2) V(50 nm)/Fe(6 ML)/MgO(2 nm), and (3) V(50 nm)/Fe(6 ML)/V(3 ML)/MgO(2 nm). The integrated total absorption and XMCD curves needed for the sum rule application are also drawn (right scale). The spectra were not corrected for the angle between the sample and the x-ray beam (45°) and for the polarization rate (40%).

$$\begin{aligned}\sigma_N &= \sigma_0 \left(1 + \frac{\text{XMCD}^{\text{tot}}}{2} \right) \\ &= \sigma_{1N}^{\text{Fe/MgO}} + \sum_{n=1}^{\infty} k^n \sigma_{1N} = \sigma_{1N}^{\text{Fe/MgO}} + \frac{k}{1-k} \sigma_{1N},\end{aligned}\quad (3)$$

$$\sigma_P = \sigma_0 \left(1 - \frac{\text{XMCD}^{\text{tot}}}{2} \right) = \sigma_{1P}^{\text{Fe/MgO}} + \frac{k}{1-k} \sigma_{1P},\quad (4)$$

where $\sigma_1^{\text{Fe/MgO}}$ is the absorption of the atomic Fe plane in contact with MgO. Using these three equations, the total XMCD signal in this particular case becomes

$$\begin{aligned}\text{XMCD}^{\text{tot}} &= \frac{\sigma_N - \sigma_P}{\sigma_0} \\ &= (1-k) \left(\frac{\sigma_{1N} - \sigma_{1P}}{\sigma_1} \right)^{\text{Fe/MgO}} + k \left(\frac{\sigma_{1N} - \sigma_{1P}}{\sigma_1} \right)^{\text{Fe}}.\end{aligned}\quad (5)$$

The terms $(\Delta\sigma_1/\sigma_1)^{\text{Fe/MgO}}$ and $(\Delta\sigma_1/\sigma_1)^{\text{Fe}}$ are no more than the equivalent XMCD signals that should be obtained for a unique atomic Fe plane in contact with MgO and in bulk Fe, respectively. As the total magnetic moment is calculated by applying the sum rules on the absorption and XMCD signals,¹¹ we thus obtain the following equation for this sample and by analogy for the others samples as

$$\langle \mu \rangle_{\text{thick Fe}} = \mu^{\text{Fe/MgO}}(1-k) + \mu^{\text{Fe}}k = 2.30 \pm 0.02 \mu_B/\text{at},\quad (6)$$

$$\begin{aligned}\langle \mu \rangle_{\text{V/Fe/MgO}} &= \frac{\mu^{\text{Fe/MgO}} + (k+k^2+k^3+k^4)\mu^{\text{Fe}} + k^5\mu^{\text{Fe/V}}}{(1+k+k^2+k^3+k^4+k^5)} \\ &= 2.23 \pm 0.04 \mu_B/\text{at},\end{aligned}\quad (7)$$

$$\begin{aligned}\langle \mu \rangle_{\text{V/Fe/V}} &= \frac{(1+k^5)\mu^{\text{Fe/V}} + (k+k^2+k^3+k^4)\mu^{\text{Fe}}}{(1+k+k^2+k^3+k^4+k^5)} = 1.68 \\ &\pm 0.04 \mu_B/\text{at},\end{aligned}\quad (8)$$

where $\langle \mu \rangle_1$ are the average magnetic moments determined by using the sum rules, $\mu^{\text{Fe/MgO}}$ and $\mu^{\text{Fe/V}}$ the magnetic moment of Fe in contact with MgO and V, and μ^{Fe} the magnetic moment of Fe surrounded by Fe. We assume that μ^{Fe} is equal to the magnetic moment of bulk Fe ($2.22 \mu_B/\text{at}$ at low temperature). The resolution of these three equations leads to the following solutions:

$$k = 0.90 \pm 0.03, \quad \text{which implies } \lambda \approx 1.5 \pm 0.5 \text{ nm},\quad (9)$$

$$\mu^{\text{Fe/MgO}} = 3.3 \pm 0.3 \mu_B/\text{at},\quad (10)$$

$$\mu^{\text{Fe/V}} = 0.7 \pm 0.3 \mu_B/\text{at}.\quad (11)$$

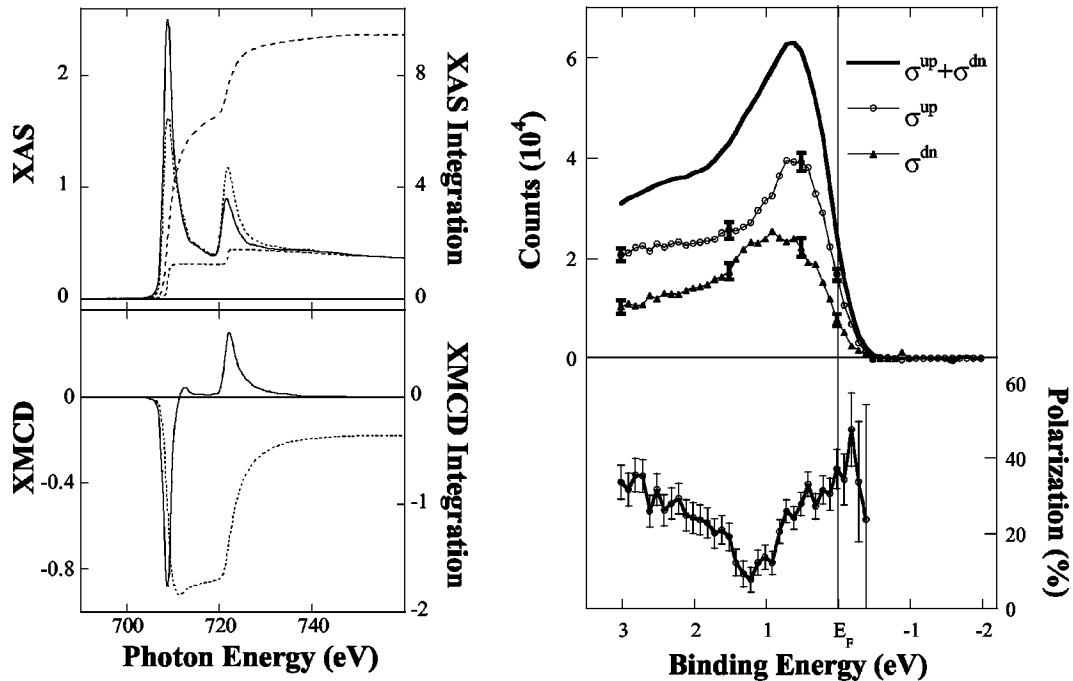


FIG. 5. Left: XMCD at the $L_{2,3}$ Fe edge obtained at remanence on a Fe/MgO (2 ML) sample (not corrected for the incident angle and polarization rate). Right: corresponding spin-integrated and spin-resolved x-ray photoemission spectra obtained with a photon energy of 500 eV (top) and corresponding polarization (bottom).

A $\mu^{\text{Fe/MgO}}$ theoretical value of $3\mu_B/\text{at}$ was predicted,⁷ whereas an experimental value of $1.34\mu_B/\text{at}$ was reported for $\mu^{\text{Fe/V}}$.²⁷ The fact that we found a higher value for $\mu^{\text{Fe/MgO}}$ and a lower one for $\mu^{\text{Fe/V}}$ is, however, not surprising. Indeed, we assume in this model that the magnetic moment of Fe was affected over only one atomic plane at the interface. This is not so sharp in practice, and a more realistic model should take into account a variation of the magnetic moment over two atomic planes for instance. In this former case, our average magnetic moments determination should lead to a slightly lower Fe magnetic moment at the interface with MgO and a much higher one at the interface with V. An asymmetry in the Fe/V and V/Fe interfaces is also possible. Again, including this effect in the calculation should lead to a much different $\mu^{\text{Fe/V}}$, but to a similar $\mu^{\text{Fe/MgO}}$. This analysis also shows that the electron escape depth is around 1.5 ± 0.5 nm in perfect agreement with the experimental determination performed by Nakajima *et al.*²⁹ on Fe (they found 1.7 ± 0.2 nm). This leads to a reasonable value for the depth of detection in XMCD measurements of 3λ (corresponding to 95% of the emitted electrons) around 4.5 ± 1.5 nm. To summarize, this analysis clearly demonstrates that the Fe magnetic moment at the interface with MgO increases up to around $3\mu_B/\text{at}$ in agreement with theory.

Finally, it should be noted that we observed no evidence at the Fe $L_{2,3}$ edges for oxidation on all the samples investigated, as expected according to the XPS analysis. One may also notice a variation of the orbital moment for the three samples (the orbital moment is proportional to the full XMCD curve's integration; see Ref. 11). However, this variation was observed to hardly depend on the way the absorption spectra were corrected for the background. A more

specific study is necessary to conclude about this point and this is not the goal of this paper.

D. Spin polarization through the MgO barrier

The XMCD and SR-XPS measurements were performed on a (001) Fe buffer layer covered by 2 ML MgO. Before starting the SR-XPS measurements at ESRF, the magnetic properties of the samples were checked by XMCD measurements performed in remanence. The magnetic moments determined by applying the sum rules were in total agreement with the previous results. We actually obtained (Fig. 5) a magnetic moment of $(2.15 \pm 0.02)\mu_B/\text{at}$ for a remanence of 94%. Thus the magnetic moment at saturation is equal to $(2.29 \pm 0.02)\mu_B/\text{at}$ to be compared to Eq. (6). In Fig. 5 are also shown the spin-integrated and spin-resolved photoemission spectra (corrected for the Sherman function) and the resulting polarization measured at room temperature. It should be noted that the reduced energy range investigated is a result of the MgO features affecting the spectra below 4 eV. A positive polarization at E_F was observed, which should lead to a positive TMR. This result is in agreement with recent TMR measurements performed on (001) Fe/MgO/Fe tunnel junctions³⁰ for which a positive TMR has been obtained.

Another important point is to compare these SR-XPS spectra of Fe covered by MgO with previous works performed on the free Fe(001) surface, in order to estimate the influence of the MgO capping. However, the comparison is pertinent only on results integrated in k space. First, it should be noted that we observed a PES signal similar to the measurement performed by angular integrated HR-UPS. This is

not surprising since first we have observed that the HR-UPS spectrum obtained on the Fe/MgO interface was not sensitive to the angular integration and second because PES spectra are not strongly different for He II or 500-eV photons in the case of $3d$ metals. It is also worth noticing that the spin-resolved density of states of the (001) Fe free surface obtained by See and Klebanoff³¹ is similar to our observations, in both shape and intensity in the range of energy investigated here (although it is difficult to compare exactly as the statistics and energy resolution are not comparable). Moreover, the calculated spin-resolved DOS proposed in this paper are clearly in good agreement with our results (at least our spin data agree better with theory than their data). There is consequently no drastic change in the k -integrated DOS when Fe is covered by MgO. The 38% polarization rate obtained here at remanence finally leads to a 42% polarization fully integrated in k space. This polarization is a little higher than the polarization measured on a free Fe surface on the same apparatus. Again, this is consistent with the calculated Fe magnetic moment at the interface with MgO which was found to be higher than on the uncovered surface.⁷ Finally, even if the electron transport in a tunnel junction is much more complex than in the Jullière approach,^{8,9} Eq. (1) gives TMR as large as 40% at room temperature using $P_1 = P_2 = 42\%$. Larger TMR values cannot be ruled out for this Fe/MgO/Fe(001) system since our polarization measurement was fully integrated in k space, whereas the current is concentrated along the [001] direction in (001) epitaxial tunnel junctions. Indeed, much larger TMR for the Fe/MgO/Fe(001) system were predicted by theory^{8,9} and recent TMR results obtained by several groups^{32,33} support this theoretical prediction.

IV. CONCLUSION

In summary, we have shown that the DOS of a metallic electrode covered by an oxide is accessible by photoemission measurements. The photoemission experiments performed on the model Fe/MgO(001) system actually allow us to clearly distinguish the Fe DOS in the MgO gap. Spin-resolved photoemission experiments were thus performed to determine the Fe polarization covered by MgO. We clearly observed that the Fe polarization found to be equal to 42% in the whole Brillouin zone was not destroyed by the top MgO barrier.

This observation was also supported by the weak hybridization between Fe and O and by the enhancement of the Fe magnetic moment at the interface with MgO, both effects being predicted by theory. Moreover, the preliminary high-resolution UPS experiments on free and MgO-covered Fe surfaces allowed us to evidence some strong modifications in the [001] direction of the Fe DOS when covered by MgO. Taking into account previous STS and SR-XPS measurements performed on the free Fe surface, these modifications may be explained by a strong decrease of the Fe minority-spin DOS near the Fermi level, in agreement with theory. Thus the 40% TMR calculated by using the fully k -integrated polarization found here is certainly a lower value for Fe/MgO/Fe tunnel junctions. The large TMR obtained recently on Fe/MgO/Fe tunnel junctions by several groups support this assumption. Spin- and angle-resolved experiments performed on the Fe/MgO(001) interface are necessary to definitely confirm this point, but the XPS and spin detector counting rates should be enhanced to reach this goal.

¹See, for instance, J. Gregg, W. Allen, N. Viart, R. Kirschman, C. Sirisathitkul, J.-P. Schille, M. Gester, S. Thompson, P. Sparks, V. Da Costa, K. Ounadjela, and M. Skvarla, *J. Magn. Mater.* **175**, 1 (1997).

²R. Stratton, *Phys. Chem. Solids* **23**, 1177 (1962).

³M. Jullière, *Phys. Lett.* **54A**, 225 (1975).

⁴S. Tehrani, E. Chen, M. Durlam, M. DeHerrera, J. M. Slaughter, J. Shi, and G. Kerszykowski, *J. Appl. Phys.* **85**, 5822 (1999); S. S. P. Parkin, K. P. Roche, M. G. Samant, P. M. Rice, R. B. Beyers, R. E. Scheuerlein, E. J. O'Sullivan, S. L. Brown, J. Bucchigano, D. W. Abraham, Y. Lu, M. Rooks, P. L. Trouilloud, R. A. Wanner, and W. J. Gallagher, *ibid.* **85**, 5858 (1999).

⁵J. L. Vassent, M. Dynna, A. Marty, B. Gilles, and G. Patrat, *J. Appl. Phys.* **80**, 5727 (1996).

⁶M. Klaua, D. Ulmann, J. Barthel, W. Wulfhelkel, J. Kirschner, R. Urban, T. L. Monchesky, A. Enders, J. F. Cochran, and B. Heinrich, *Phys. Rev. B* **64**, 134411 (2001).

⁷C. Li and A. J. Freeman, *Phys. Rev. B* **43**, 780 (1991).

⁸W. H. Butler, X. G. Zhang, T. C. Schulthess, and S. M. MacLaren, *Phys. Rev. B* **63**, 054416 (2001).

⁹J. Mathon and A. Umerski, *Phys. Rev. B* **63**, 220403 (2001).

¹⁰Vassent *et al.* (Ref. 5) have observed some Fe intermixing in MgO, a result *a priori* in contradiction with our results. How-

ever, they observed this effect during the MgO growth on a heated Fe buffer layer, whereas we first grew the MgO layer at room temperature and heated the system after the growth process. Since we did not observe any interdiffusion up to 870 K, it means that the intermixing observed by Vassent *et al.* was probably due to Fe segregation (or associated kinetic effect at the surface) during the growth rather than interdiffusion.

¹¹C. T. Chen, Y. U. Idzerda, H.-J. Lin, N. V. Smith, G. Meigs, E. Chaban, G. H. Ho, E. Pellegrin, and F. Sette, *Phys. Rev. Lett.* **75**, 152 (1995).

¹²L. E. Klebanoff, D. G. Van Campen, and R. J. Pouliot, *Rev. Sci. Instrum.* **64**, 2863 (1993).

¹³G. Ghiringhelli, K. Larsson, and N. B. Brookes, *Rev. Sci. Instrum.* **70**, 4225 (1999).

¹⁴It should be noted that a carbon contamination of (001) Fe surface leads to a $c2 \times 2$ surface structure. In this case, a square lattice is also found and should not be identified as the 1×1 (001) Fe surface lattice turned by 45° with this $c2 \times 2$ square lattice. Thus, if there is no C and consequently no $c2 \times 2$ surface structure, the diffraction patterns in RHEED are similar on MgO and Fe(001) surface (2D diffraction, no extinction in the reciprocal lattice of Fe). However, they are different in LEED (3D diffraction) due to the extinction of (hkl) contribution of Fe for $h+k$

- $+l=2p+1$. When the $c2\times 2$ surface structure is present on the Fe surface, additional streaks are observed by RHEED along the [110] azimuth, and the reciprocal lattices of Fe+C and MgO become identical in LEED.
- ¹⁵J. L. Vassent, A. Marty, B. Gilles, and C. Chatillon, *J. Cryst. Growth* **219**, 434 (2000); **219**, 444 (2000).
- ¹⁶T. Kanaji, T. Kagotani, and S. Nagata, *Thin Solid Films* **32**, 217 (1976). T. Urano and T. Kanaji, *J. Phys. Soc. Jpn.* **57**, 3043 (1988).
- ¹⁷P. C. J. Graat and M. A. J. Somers, *Appl. Surf. Sci.* **100**, 36 (1996).
- ¹⁸H. L. Meyerheim, R. Popescu, J. Kirschner, N. Jedrecy, M. Sauvage-Simkin, B. Heinrich, and R. Pinchaux, *Phys. Rev. Lett.* **87**, 076102 (2001).
- ¹⁹B. T. Jonker, K. H. Walker, E. Kisher, G. A. Prinz, and C. Carbone, *Phys. Rev. Lett.* **57**, 142 (1986).
- ²⁰N. B. Brookes, A. Clarke, P. D. Johnson, and M. Weinert, *Phys. Rev. B* **41**, 2643 (1990).
- ²¹C. Carbone, R. Rochow, L. Braicovich, R. Jungblut, T. Kachel, D. Tillman, and E. Kisker, *Phys. Rev. B* **41**, 3866 (1990).
- ²²E. Vescovo, O. Rader, and C. Carbone, *Phys. Rev. B* **47**, 13 051 (1993).
- ²³M. Sawada, A. Kimura, and A. Kakizaki, *Solid State Commun.* **109**, 129 (1999).
- ²⁴J. A. Stroscio, D. T. Pierce, A. Davies, and R. J. Celotta, *Phys. Rev. Lett.* **75**, 2960 (1995). P. D. Johnson, Y. Chang, N. B. Brookes, and M. Weinert, *J. Phys.: Condens. Matter* **10**, 95 (1998).
- ²⁵W. A. Hofer, J. Redinger, A. Biederman, and P. Varga, *Surf. Sci.* **482**, 1113 (2001).
- ²⁶S. Ohnishi, A. J. Freeman, and M. Weinert, *Phys. Rev. B* **28**, 6741 (1983).
- ²⁷A. Scherz, H. Wende, P. Pouloupoulos, J. Lindner, K. Baberschke, P. Blomquist, R. Wäppling, F. Wilhelm, and N. N. Brookes, *Phys. Rev. B* **64**, 180407 (2001).
- ²⁸P. Turban, F. Dulot, B. Kierren, and S. Andrieu, *Appl. Surf. Sci.* **177**, 282 (2001).
- ²⁹R. Nakajima, J. Stöhr, and Y. U. Idzerda, *Phys. Rev. B* **59**, 6421 (1999).
- ³⁰E. Popova, J. Faure-Vincent, C. Tiusan, C. Bellouard, H. Fischer, M. Hehn, F. Montaigne, M. Alnot, S. Andrieu, A. Schuhl, E. Snoeck, and V. Da Costa, *Appl. Phys. Lett.* **81**, 1035 (2002).
- ³¹A. K. See and L. E. Klebanoff, *J. Appl. Phys.* **79**, 4796 (1996). L. E. Klebanoff, D. G. Van Campen, and R. J. Pouliot, *Rev. Sci. Instrum.* **64**, 2863 (1993).
- ³²M. Bowen, V. Cros, F. Petroff, A. Fert, C. Martínez Boubeta, J. L. Costa-Krämer, J. V. Anguita, A. Cebollada, F. Briones, J. M. de Teresa, L. Morellón, M. R. Ibarra, F. Güell, F. Peiró, and A. Cornet, *Appl. Phys. Lett.* **79**, 1655 (2001).
- ³³J. Faure-Vincent, C. Tiusan, E. Jouguelet, F. Canet, M. Sajiedine, C. Bellouard, E. Popova, M. Hehn, F. Montaigne, and A. Schuhl, *Appl. Phys. Lett.* **82**, 4507 (2003).